TOMOGRAPHY® RESEARCH ARTICLE

Bias in PET Images of Solid Phantoms Due to CT-Based Attenuation Correction

Darrin W. Byrd[1], John J. Sunderland[2], Tzu-Cheng Lee[1], and Paul E. Kinahan[1]

[1]Department of Radiology, University of Washington, Seattle, WA; and [2]Department of Radiology, University of Iowa, Iowa City, IA

Corresponding Author:
Paul E. Kinahan, PhD
206-543-0236, University of Washington,
Box 357987, Seattle, WA 98195;
E-mail: kinahan@uw.edu

Key Words: PET, calibration, phantoms
Abbreviations: Computed tomography (CT), positron emission tomography (PET), Germanium isotope 68 (^{68}Ge), Computerized Imaging Reference Systems, Incorporated (CIRS), Image quality phantom (IQ), kilovolt potential (kVp), National Electrical Manufacturers Association (NEMA)

ABSTRACT

The use of computed tomography (CT) images to correct for photon attenuation in positron emission tomography (PET) produces unbiased patient images, but it is not optimal for synthetic materials. For test objects made from epoxy, image bias and artifacts have been observed in well-calibrated PET/CT scanners. An epoxy used in commercially available sources was infused with long-lived ^{68}Ge/^{68}Ga nuclide and measured on several PET/CT scanners as well as on older PET scanners that measured attenuation with 511-keV photons. Bias in attenuation maps and PET images of phantoms was measured as imaging parameters and methods varied. Changes were made to the PET reconstruction to show the influence of CT-based attenuation correction. Additional attenuation measurements were made with a new epoxy intended for use in radiology and radiation treatment whose photonic properties mimic water. PET images of solid phantoms were biased by between 3% and 24% across variations in CT X-ray energy and scanner manufacturer. Modification of the reconstruction software reduced bias, but object-dependent changes were required to generate accurate attenuation maps. The water-mimicking epoxy formulation showed behavior similar to water in limited testing. For some solid phantoms, transformation of CT data to attenuation maps is a major source of PET image bias. The transformation can be modified to accommodate synthetic materials, but our data suggest that the problem may also be addressed by using epoxy formulations that are more compatible with PET/CT imaging.

INTRODUCTION

With proper calibration, positron emission tomography (PET) accurately quantifies the concentration of radiolabeled molecules in patients noninvasively and with excellent sensitivity. Biomarkers computed from these measured concentrations have proven utility in managing the treatment of certain cancers (1-4). However, the acquisition of PET data is a physically complicated process, and the software required to convert the raw data to form an image relies on numerous approximations and empirical corrections. Poor calibration or nonoptimal processing of the data leads to biased images (5-7). This bias may reduce PET's prognostic value for patients and researchers (8).

One of the most important effects that the reconstruction must model is the interaction of 511-keV annihilation photons with tissues (in patients) or other materials (in calibration objects, which are commonly called "phantoms"). Without mathematical corrections, absorption of photons leads to reduced signal from central regions of PET images as well as edge artifacts. Scattered photons also affect raw PET data because PET's coincidence detection, which does not use physical collimation, cannot distinguish between scattered and unscattered photons for small deflections and therefore misplaces them in the raw projection data.

For modern PET scanners, the corrections for scattered and absorbed photons are calculated from computed tomography (CT) images that are acquired just before or after the PET scan (9, 10). CT volume images are mapped to attenuation images, commonly via a piecewise-linear transformation (11), whose final units are "attenuation coefficients" that represent the probability of an annihilation photon being "attenuated" (absorbed or scattered) per unit length. With these attenuation images, the scanner is able to estimate the required data corrections for scatter and absorption that are applied during the reconstruction.

However, CT-based attenuation correction suffers from a known limitation in that there is no unique relationship between CT pixelwise image values (Hounsfield Units) and attenuation coefficients at the energy of PET photons. Figure 1 shows this problem. The disparity in the absorption properties of bone and soft tissue varies with photon energy, and it is much greater at lower CT photon energies than at PET energy. The piecewise-linear transformation succeeds in producing sufficiently accu-

ISSN 2379-1381 http://dx.doi.org/10.18383/j.tom.2018.00043

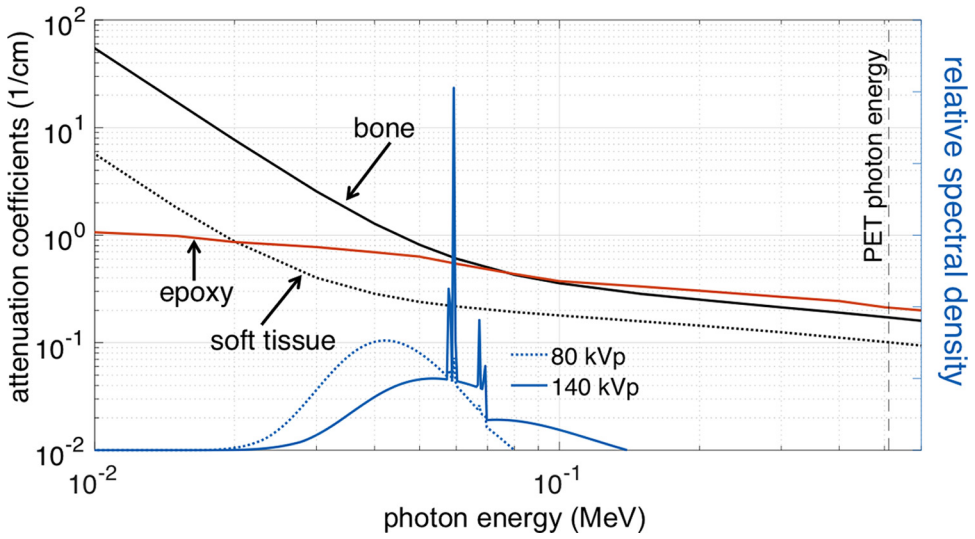

Figure 1. Attenuation coefficients for bone and soft tissues (black lines) and filtered bremsstrahlung spectra for 80- and 140-kVp computed tomography (CT) scans (blue lines). Tissue attenuation values are from the National Institute of Standards and Technology (12). X-ray energies are from the Catsim software package (13). Epoxy composition is from the PubChem database (14).

rate attenuation images because human tissues have predictable chemical compositions and their CT image values can be coarsely grouped into soft tissue and bone. This allows bone to be scaled separately, thus avoiding overestimation of Compton scatter at PET's 511-keV energy. Figure 2 shows a continuous, piecewise-linear transformation used in a modern PET/CT scanner.

Tests of quantitative accuracy for PET scanners often involve phantoms that are carefully designed to validate a PET/CT scanner's correction of all physical effects, including detection sensitivity and random coincidences (15, 16). Among current published standards and accreditation organizations, water-filled phantoms containing short-lived radionuclides predominate (17, 18). These phantoms' physical properties are well-matched to patient scans, to the extent that water-filled phantom scans are routinely used to measure the calibration factors used to convert clinical scans from a scanner's arbitrary units to true nuclide concentration. However, recent reports suggest that this calibration process may result in increased variability in PET signal, likely owing to difficulties in repeatedly refilling short-lived phantoms each time the phantom is used (19).

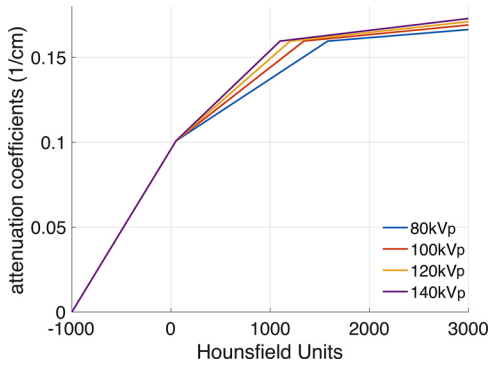

Figure 2. Estimated attenuation coefficients at 511 keV versus Hounsfield Units from CT images with varying characteristic voltage. Coefficients were copied from a modern clinical positron emission tomography (PET)/CT scanner.

This problem can potentially be solved by using phantoms infused with long-lived radionuclides, which can be measured repeatedly without refilling. These phantoms follow highly predictable decay curves, allowing bias to be computed at multiple time points with fewer confounding factors. In this work, we investigate an important drawback of long-lived phantoms: they are usually constructed from solid materials to mitigate the risk of spilling, and these solid materials have attenuation properties that are not accurately estimated by the CT-based attenuation estimation used for human tissues (Figure 2). This can lead to image bias. Below, we examine the bias in attenuation images and reconstructed PET images of several solid long-lived phantoms, and we show that CT-based attenuation correction underestimates photon absorption by the epoxy used in their construction.

METHODOLOGY

Phantoms were constructed using epoxy with and without the admixture of long-lived positron-emitting ^{68}Ge/^{68}Ga (^{68}Ge). Phantoms were imaged by PET/CT and by 511-keV transmission scans. Modifications to the X-ray tube voltage and reconstruction software were used to investigate the dependence of PET image bias on CT-based attenuation correction.

Image Quality Phantom

A National Electrical Manufacturers Association (NEMA) Image Quality (IQ) phantom (15) (Data Spectrum Corporation, Durham, NC) was filled with solid epoxy and ^{68}Ge at an initial background concentration of 7.19 kBq/mL. The phantom, shown in Figure 3A, contained spherical inserts at the sizes specified in the NEMA test standard, but with the modification that all spheres were filled to the same concentration of radionuclide (ie, the phantom contained no nonradioactive spheres). Sphere contrast was 7.7:1 relative to background, and the same epoxy formula was used to fill both background and spheres. The phantom was scanned on 3 commercial PET/CT scanners: a Discovery STE (General Electric Healthcare, Waukesha, WI), a

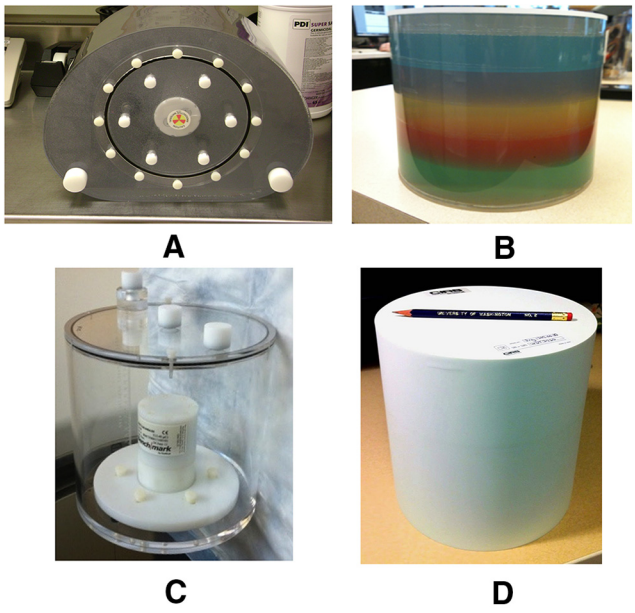

Figure 3. Image Quality (IQ) phantom filled with epoxy infused with ^{68}Ge (A). Nonradioactive epoxy phantom made from the same epoxy as the IQ phantom and the X-Cal phantom (B). X-Cal phantom mounted for scanning in an American College of Radiology flood phantom (C). CIRS 20cm *Plastic Water LR* phantom (D).

Biograph (Siemens Healthcare, Knoxville, TN), and a Philips Gemini TF Big Bore (Philips Healthcare, Best, The Netherlands.). The dependence of reconstructed signal on CT X-ray energy (commonly characterized by the potential in kilovolts [kVp] applied to the X-ray tube) and variations in the reconstruction software were investigated.

Nonradioactive Epoxy Phantom

A 20-cm cylinder (Figure 3B) was filled with the same epoxy used in the IQ phantom, but without the addition of any radionuclide. This phantom was scanned on a General Electric Discovery LS and a Siemens HR+. Both scanners used positron sources to measure photon absorption at the same energy measured in clinical PET scans, 511 keV. Filtered backprojection was used to generate attenuation images. The phantom was also CT-scanned on the General Electric Discovery STE scanner, and attenuation images resulting from 80-, 100-, 120-, and 140-kVp CT scans were copied from the scanner console and read in MATLAB (MathWorks, Natick, MA).

X-Cal Phantom

A comercially-available 45-mm cylinder phantom was scanned inside a 20-cm water-filled American College of Radiology flood phantom (Figure 3C) on the same Discovery STE as the IQ phantom. The 45-mm phantom is sold as part of a "cross-calibration" kit sold by RadQual, LLC (Weare, NH) and we consequently refer it to it as the X-Cal phantom. It was made from the same epoxy as the above sources. We have previously reported on its signal properties and the bias between measured values and known tracer concentration (19, 20).

Nonradioactive PlasticWater Phantom

A nonradioactive 20-cm-diameter cylinder (Figure 3D) was constructed from a different epoxy that was formulated to better match the attenuation properties of human tissues. The cylinder

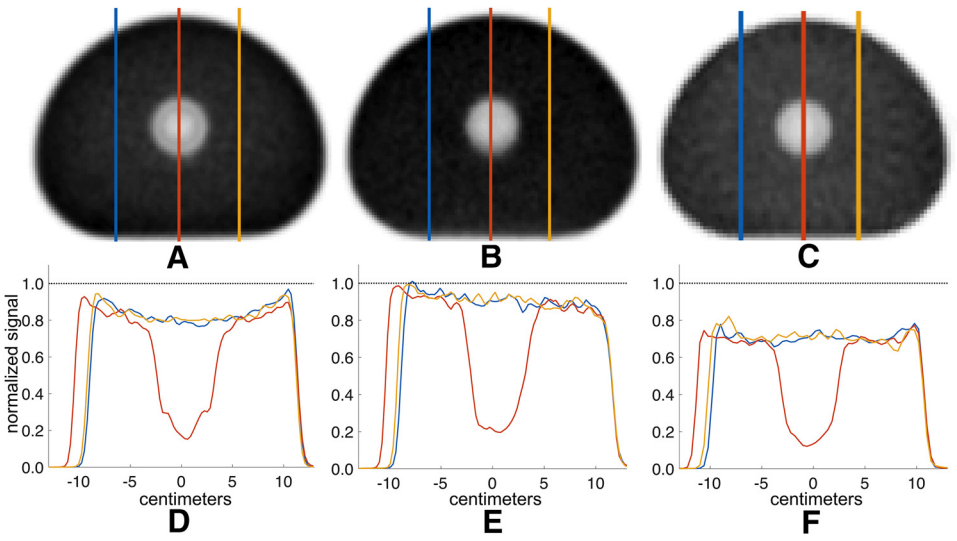

Figure 4. Images and profiles of PET signal from the IQ phantom in three scanners. Signal has been normalized by the known nuclide concentration, with truth represented by the horizontal black dotted line. The 3 columns show scanner models from 3 manufacturers: a General Electric Discovery STE (A and D), a Siemens Biograph (B and E), and a Philips Gemini TF Big Bore (C and F). Data were averaged over 3 cm axially and acquired over a decay-compensated duration of 60 minutes. Colored lines in the images correspond to the locus of points shown in the profiles. Color windows are matched between images.

Table 1. PET Signal (measured/known) in the Background Region of the IQ Phantom with Varying X-ray Tube Voltage and Modified CT Rescaling for 2 of the Scanners in this Study

kVp	Siemens	General Electric
80	0.92	0.75
100	0.97	0.78
120	0.95	0.80
140	0.95	0.82
120 (mod'd AC)		1.04

was constructed by Computerized Imaging Reference Systems, Incorporated, or CIRS (Norfolk, VA), and was filled with their "LR" epoxy. The phantom was scanned on a General Electric Discovery LS to generate 511-keV transmission images as well as CT-based attenuation images.

Variations in Imaging Parameters

CT photon energies were varied by changing the X-ray voltage in CT scans of the IQ phantom and the nonradioactive phantoms. CT voltage modifications were done using the scanners' user-facing interfaces and spanned the available settings of 80, 100, 120 and 140 kVp. Where possible, the impact of CT voltage on PET measured radioactivity concentration was assessed.

Modification of CT-Based Attenuation Correction

An additional variation for the data measured on the General Electric Discovery STE scanner was the modification of the rescaling functions shown in Figure 2 to provide more accurate conversion of the CT images to attenuation images for the IQ and X-Cal phantoms. In particular, for the domain that contained the phantoms' image values of ~80–90 Hounsfield Units, the rescaling coefficient (slope) for 120-kVp CT images was increased. The new coefficients for the 2 phantoms were chosen to make the resulting attenuation images agree with values obtained from the 511-keV transmission scans of the phantoms. Modifications to the attenuation conversion were made in MATLAB, and reconstructions were performed using code from General Electric.

RESULTS

The IQ phantom PET images demonstrated quantitative bias. For all 3 PET/CT scanners, the bias was spatially variable. Figure 4 shows data from axially averaged (ie, thick-slice) images from the 3 scanners. For each scanner, the figure depicts data from ~60-minutes' worth of scanning (scan durations were corrected to a common time point to compensate for phantom decay).

Table 1 shows the PET background signal divided by the known nuclide concentration for the images in Figure 4. Background signal was computed as in the NEMA standard using 28-mm regions (15).

Figure 5 shows the attenuation image from the transmission scan of the nonradioactive epoxy phantom (Figure 3B) on the GE Discovery LS. The values obtained on the Siemens HR+ were similar. Figure 5 also shows profiles through this transmission image as well as the attenuation values that were estimated from CT data on the General Electric Discovery STE. The profiles show that the CT-based attenuation images do not agree with the values obtained using positron annihilation photons. While varying X-ray tube voltage does lead to varying CT signal, no user-selectable tube voltage led to agreement between the CT-based attenuation images and the transmission image. Region of interest means in the CT-based attenuation images were 0.095, 0.096, 0.097, and 0.098 cm^{-1} as the CT voltage varied. In the transmission scan, the value was 0.105 cm^{-1}.

Figure 6A shows the attenuation images generated in the reconstruction before and after our modification of the algorithm. Figure 6B, shows PET data reconstructed with each attenuation image. It can be seen that the accuracy of the signal is improved. The bottom row of Table 1 shows that the modifications to the attenuation correction lead to more accurate PET signal.

Figure 7A shows a transaxial slice containing the spherical inserts in an image made with the modified attenuation correction algorithm. Figure 7B shows mean signal from regions of interest drawn on the spheres. Averaged over sphere sizes, the signal was 1.20 times larger in the images with modified attenuation correction, indicating that if solid phantoms are used for

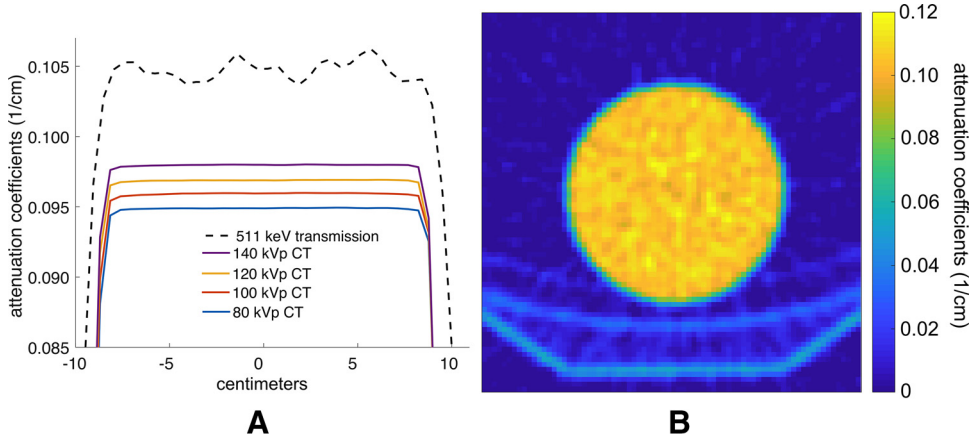

Figure 5. Profiles showing CT-based attenuation estimates in the solid epoxy phantom as well as 511-keV transmission measurement (dashed line) (A).The attenuation image produced using 511-keV photons (B).

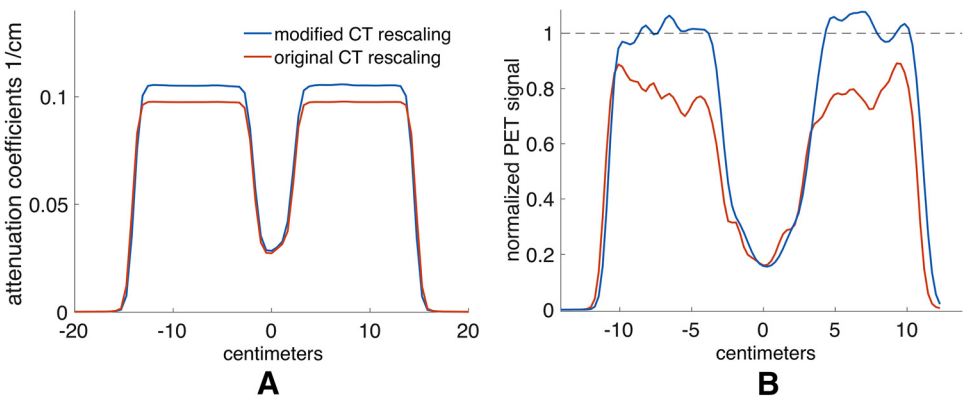

Figure 6. Profiles through CT-based attenuation images before and after our modifications to the CT attenuation correction algorithm (A). Profiles through the reconstructed PET images made with the pre- and postmodification attenuation data, showing improved signal accuracy (B). PET signal has been divided by known phantom background activity concentration.

resolution measurements, some compensation for attenuation bias must be applied.

Figure 8 shows the signal from PET images of the X-Cal source before and after modification to the attenuation correction. With the modified algorithm, the signal is visibly more accurate. Using XCaliper (20), a previously reported method for drawing regions of interest in the X-Cal phantom, the bias was measured as −4.7% using the standard attenuation correction algorithm and 0.5% with our modifications. Different scale factors were used in the respective modifications to the CT rescaling for the X-Cal and IQ phantoms.

Figure 9 shows profiles through transmission scans of the PlasticWater epoxy phantom and a similarly sized water-filled cylinder. Also shown are CT-based attenuation estimates. It can be seen that the PlasticWater epoxy better matches the water values in the transmission scans. In addition, the bias between the transmission scan and the CT-based attenuation images is similar to that seen in an actual water phantom, as Table 2 also shows.

DISCUSSION

Inaccuracy of PET activity concentration measurements in solid epoxy phantoms has been previously observed and is a challenge to their use in determining scanner calibration accuracy. We have investigated signal bias in solid phantoms made from an epoxy that is used in commercially available sources. While several factors may affect long-lived phantom bias, such as scatter correction and prompt gamma emission by ^{68}Ge, our results show that bias is greatly reduced by modification to the CT-based attenuation correction algorithm.

Although we did not evaluate attenuation images for all scanners used, Figure 4 shows that each scanner exhibited signal bias over all or part of the phantom images. It is expected that scanners from different manufacturers would behave similarly, as the generation of X-rays, and therefore the transformation needed to generate attenuation images, is substantially similar across scanner types (9).

The transmission measurements made with 511-keV photons provide a more accurate estimate of attenuation because, in contrast to CT photons, their probability of various modes of scatter interactions (ie, Compton, photoelectric, Rayleigh) is precisely the same as for the photons emitted during a PET scan. Figure 5A shows that regardless of X-ray energy, the CT-based attenuation values have a negative bias versus the transmission scan. Because the PET reconstruction uses these attenuation values to compensate for lost photons, we would expect PET images of the phantom to inherit this negative bias, as was observed. While the PET image bias does change with CT values, as shown in Table 1, X-ray energy cannot be varied arbitrarily and no user-selectable setting led to unbiased PET images.

As Figures 6B and 8 and Table 1 show, modifying the reconstruction to improve the accuracy of attenuation images leads to more accurate PET measurements and reduced bias. Figure 7B shows that recovery curves, which are used to char-

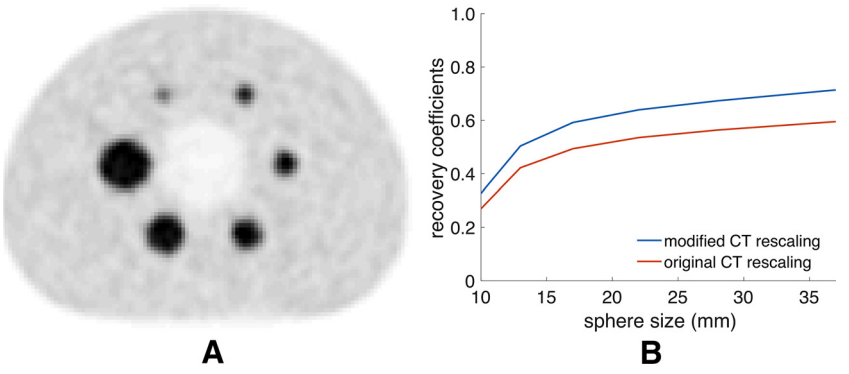

Figure 7. IQ phantom reconstructed with modified CT-based attenuation correction, showing uniformity in the background region (A). Mean region of interest divided by known concentration (signal recovery) for the depicted spheres (B).

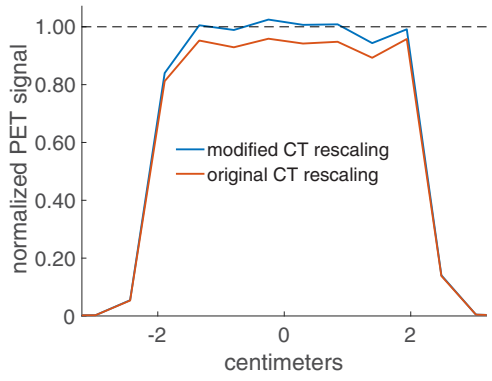

Figure 8. PET signal from the 45-mm-diameter X-Cal phantom divided by known phantom activity concentration. Here, the modified attenuation correction used slightly different scaling than was used for the IQ phantom reconstructions.

acterize resolution, also exhibit reduced bias when attenuation correction is accurate.

The precise modifications required to generate accurate attenuation images were object-dependent. For the IQ phantom and the X-Cal phantom, the correct coefficient was determined by measuring the Hounsfield Units of the epoxy in each scan and choosing the new slope of the rescaling formula that led to 0.105 1/cm. The IQ and X-Cal phantoms had Hounsfield Units of 92.1 and 82.2, respectively, although they were made of the same material. We did not attempt to correct the CT transformation for multiple X-ray tube voltages, but we note that because CT values themselves depend on voltage, the optimal modifications for one voltage will not work for others. We further expect that they would change if the experiment were repeated with a different epoxy. In all, this indicates that correcting bias in epoxy with this method would require premeasured look-up tables so that the appropriate rescaling factors are available for a range of scan scenarios.

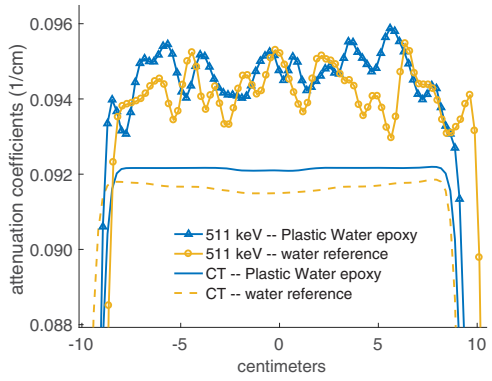

Figure 9. Profiles through 511-keV transmission scans and standard CT-based attenuation images for the PlasticWater LR phantom and a similarly sized water phantom.

Table 2. Attenuation Values (1/cm) Measured by Large Regions of Interest in the PlasticWater LR phantom and Similarly Sized Aqueous Phantom from CT Scans (First 4 Rows) and Transmission Measurements (Bottom Row)

	LR	Water
80 kVp	0.0922	0.0917
100 kVp	0.0922	0.0916
120 kVp	0.0921	0.0916
140 kVp	0.0922	0.0916
511 keV trans	0.0949	0.0944

An alternative approach would be the use of an epoxy whose attenuation properties are better suited to the transformation used by the scanner. The PlasticWater phantom was investigated with this in mind. As Table 2 shows, the attenuation estimates from a GE Discovery LS do not show a dependence on X-ray tube voltage, and the bias of attenuation estimates versus the transmission scan is reduced. Further, the bias between CT-based and 511-keV transmission measurements closely resembles that of an actual water phantom (Figure 9), for which the scanner's reconstruction algorithm is presumably well-calibrated. That is, the slight bias of CT-based water attenuation coefficients may be intentionally introduced to compensate for other approximations in the algorithm, such as imperfect scatter correction. It is therefore plausible, although not confirmed here, that a radioactive PET phantom constructed from the PlasticWater epoxy would exhibit bias similar to a water-filled phantom.

We emphasize that bias in attenuation estimates of our solid phantoms made from CT images (Figure 5A) does not imply that clinical patient images are similarly affected. Rather, it is a property of an empirical optimization in the reconstruction that favors clinical patient images over other materials.

While our study was limited in scope, using a small number of scanners, we expect that the bias seen in our PET images could be replicated on most scanners using CT-based attenuation correction, owing to the similarity in the way their X-rays are generated and detected.

Future work should better characterize the robustness and trade-offs of applying software modifications versus using new materials for phantom construction. In particular, the fabrication of long-lived radioactive phantoms can present unique manufacturing challenges, and the authors make no claims about the fitness of the specific materials used in the present study for this purpose. Software modifications would require vendor participation, but have the advantage of being compatible, in principle, with any existing phantom whose attenuation properties are known. Standardization of phantom size and composition may lead to object-dependence being a smaller hurdle for software-based bias reduction.

CONCLUSIONS

Solid, long-lived PET phantoms can suffer signal bias owing to physical factors. We have shown that corrections for photon attenuation computed from CT images can be a significant source of bias. Modifications to the reconstruction algorithm can reduce the errors in CT-based attenuation estimates, although the required parameters are likely to depend on X-ray tube voltage, the type of epoxy used, and the geometry of the phantom. The use of epoxy that better matches the photon-scattering properties of water appears to be a promising alternative to algorithmic corrections if they can be manufactured reliably, which is a nontrivial task.

ACKNOWLEDGMENTS

This work was supported by NIH-SAIC Contract 24XS036-004, NIH Grant R01CA169072, and NIH Grant U01 CA148131. The authors would like to thank Adam Strohn, Levent Sensoy, Joshua Scheuermann, and Joel Karp for their help in coordinating phantom transfers and acquiring data, and Steve Kohlmeyer and Keith Allberg for their assistance with phantom construction and testing.

Disclosure: Dr. Kinahan reports grants from NIH, during the conduct of the study; other from PET/X LLC, outside the submitted work; and Research Grant from GE Healthcare.

REFERENCES

1. Avril N, Sassen S, Schmalfeldt B, Naehrig J, Rutke S, Weber WA, Werner M, Graeff H, Schwaiger M, Kuhn W. Prediction of response to neoadjuvant chemotherapy by sequential F-18-fluorodeoxyglucose positron emission tomography in patients with advanced-stage ovarian cancer. J Clin Oncol. 2005;23:7445–7453.
2. Weber WA. Assessing tumor response to therapy. J Nucl Med. 2009;50 (*Suppl* 1):1S–10S.
3. Fletcher JW, Djulbegovic B, Soares HP, Siegel BA, Lowe VJ, Lyman GH, Coleman RE, Wahl R, Paschold JC, Avril N, Einhorn LH, Suh WW, Samson D, Delbeke D, Gorman M, Shields AF. Recommendations on the use of 18F-FDG PET in oncology. J Nucl Med. 2008;49:480–508.
4. Shankar LK, Hoffman JM, Bacharach S, Graham MM, Karp J, Lammertsma AA, Larson S, Mankoff DA, Siegel BA, Van DA, Annick VdA, Yap J, Sullivan D. Consensus recommendations for the use of 18F-FDG PET as an indicator of therapeutic response in patients in national cancer institute trials. J Nucl Med. 2006;47: 1059–1066.
5. Kinahan PE, Fletcher JW. PET/CT standardized uptake values (SUVs) in clinical practice and assessing response to therapy. Semin Ultrasound CT MR. 2010;31: 496–505.
6. Boellaard R. Standards for PET image acquisition and quantitative data analysis. J Nucl Med. 2009;50:11S–20S.
7. Kumar V, Nath K, Berman CG, Kim J, Tanvetyanon T, Chiappori AA, Gatenby RA, Gillies RJ, Eikman EA. Variance of standardized uptake values for FDG-PET/CT greater in clinical practice than under ideal study settings. Clin Nucl Med. 2013;38:175–182.
8. Kurland BF, Doot RK, Linden HM, Mankoff DA, Kinahan PE. Multicenter trials using 18F-fluorodeoxyglucose (FDG) PET to predict chemotherapy response: effects of differential measurement error and bias on power calculations for unselected and enrichment designs. Clin Trials. 2013;10:886–895.
9. Carney JPJ, Townsend DW, Rappoport V, Bendriem B. Method for transforming CT images for attenuation correction in PET/CT imaging. Med phys. 2006;33: 976–983.
10. Kinahan PE, Townsend DW, Beyer T, Sashin D. Attenuation correction for a combined 3D PET/CT scanner. Med Phys. 1998;25:2046–2053.
11. Abella M, Alessio AM, Mankoff DA, MacDonald LR, Vaquero JJ, Desco M, Kinahan PE. Accuracy of CT-based attenuation correction in PET/CT bone imaging. Phys Med Biol. 2012;57:2477–2490.
12. Hubbell JH, Seltzer M. Tables of X-Ray Mass Attenuation Coefficients and Mass Energy-Absorption Coefficients (version 1.4). National Institute of Standards and Technology: Gaithersburg, MD.
13. De Man B, Basu S, Chandra N, Dunham B, Edic P, Iatrou M, McOlash S, Sainath P, Shaughnessy C, Tower B. CatSim: a new computer assisted tomography simulation environment. *Proceedings Volume 6510, Medical Imaging 2007: Physics of Medical Imaging , 65102G*; 2007.
14. NCFBI. PubChem Compound Database; CID=169944.
15. Daube-Witherspoon ME, Karp JS, Casey ME, DiFilippo FP, Hines H, Muehllehner G, Simcic V, Stearns CW, Adam L-E, Kohlmyer S. PET performance measurements using the NEMA NU 2-2001 standard. J Nucl Med. 2002;43:1398–1409.
16. Scheuermann JS, Reddin JS, Opanowski A, Kinahan PE, Siegel BA, Shankar LK, Karp JS. Qualification of national cancer institute-designated Cancer Centers for Quantitative PET/CT Imaging in Clinical Trials. J Nucl Med. 2017;58:1065–1071.
17. Boellaard R, Delgado-Bolton R, Oyen WJG, Giammarile F, Tatsch K, Eschner W, Verzijlbergen FJ, Barrington SF, Pike LC, Weber WA. FDG PET/CT: EANM procedure guidelines for tumour imaging: version 2.0. Eur J Nucl Med Mol Imaging. 2015;42:328–354.
18. Doot RK, Scheuermann JS, Christian PE, Karp JS, Kinahan PE. Instrumentation factors affecting variance and bias of quantifying tracer uptake with PET,âïCT. Med Phys. 2010;37:6035–6046.
19. Byrd D, Christopfel R, Arabasz G, Catana C, Karp J, Lodge MA, Laymon C, Moros EG, Budzevich M, Nehmeh S, Scheuermann J, Sunderland J, Zhang J, Kinahan P. Measuring temporal stability of positron emission tomography standardized uptake value bias using long-lived sources in a multicenter network. J Med Imaging. 2018;5:011016.
20. Byrd DW, Doot RK, Allberg KC, MacDonald LR, McDougald WA, Elston BF, Linden HM, Kinahan PE. Evaluation of cross-calibrated (68)Ge/(68)Ga phantoms for assessing PET/CT measurement bias in oncology imaging for single- and multicenter trials. Tomography. 2016;2:353–360.